Available online at www.sciencedirect.com
SCIENCE DIRECT®
International Journal of Thermal Sciences 45 (2006) 841–847
International Journal of Thermal Sciences
www.elsevier.com/locate/ijts

Study of the temperature field in microchannels of a PDMS chip with embedded local heater using temperature-dependent fluorescent dye

R. Fu, B. Xu, D. Li *

Department of Mechanical and Industrial Engineering, University of Toronto, 5 King's College Road, Toronto, ON, Canada M5S 3G8

Received 20 April 2005; accepted 15 November 2005

Available online 18 January 2006

Abstract

This paper presents a simple microheater design for microfluidic devices by embedding resistance wire into a PDMS chip, and the results of an experimental study of the thermal response of liquid samples in the PDMS chip with the embedded local heater. Temperature-dependent fluorescent dye was used to measure the temperature distribution within a microchannel heated by the local heater. Two heater configurations were built, tested, and compared with numerical simulation. Through comparing the performance of these two configurations, heating and cooling rates and the characteristics of the temperature field were evaluated. Additionally, thermal cycling at two different temperature levels was achieved by controlling the power of the local heater.

Keywords: Microfluidics; Microheater; Microreactor; Temperature measurement; Fluorescent dye

1. Introduction

Interest in microfluidic lab-on-a-chip devices is largely motivated by the extensive potential applications. These integrated, miniaturized devices promise to offer many advantages over conventional bench-top analytical and synthesizing instruments, such as increased efficiency, high throughput, portability, sensitive process control, reduced reagent/sample consumption, and reduced analysis time and cost [1–5]. Advanced fabrication technologies make it possible to develop more complicated microfluidic devices with versatile applications.

Control of fluid temperatures during analysis is often important, particularly during reaction and separation. Chemical synthesis in microreactors requires controlled heating/incubation in combinatorial chemical reactions, and the reviews can be found elsewhere [6]. The use of incubating microreactors has also been reported to investigate reaction kinetics [7], cell-free protein synthesis [8], and nanocrystal growth [9].

Many lab-on-chip devices also require thermal control. Prior to genetic analysis, DNA must first be extracted from cells. This can be accomplished through the destruction of the cell membrane (cytolysis) by heating the cell [10]. The DNA is then amplified through polymerase chain reaction (PCR), which needs precise thermal cycling at different temperature levels [11,12]. The cycling process can be done more rapidly in a microfluidic system than in a conventional system due to smaller sample volumes. Thermal cycling is also required for generating microbubbles for micromixing [13] and DNA sample transport [14].

In present technologies, the following methods have been applied to provide heating for microdevices. Generally, electric resistance microheaters are patterned onto a glass or silicon wafer surface using microfabrication technology [15–17], and a glass or silicon chip with a microchannel is bonded onto the surface, so that the microheaters can heat the fluid in the microchannel. The microchannel is either molded into a polymer [6,18], etched into glass [11], or fabricated from photoresist [19]. Joule heating, which results from current passing through a solution via electrodes, has been investigated as a means of heating [20]. The use of Peltier heaters in contact with the microchannel substrate has also been reported [12,21]. Among these methods, using a microheater is the most attractive because it can be made very small and can be integrated with other circuits. However, the design and fabrication of micro-

* Corresponding author. Fax: +1 416 978 7753.
E-mail address: dli@mie.utoronto.ca (D. Li).

1290-0729/$ – see front matter
doi:10.1016/j.ijthermalsci.2005.11.009

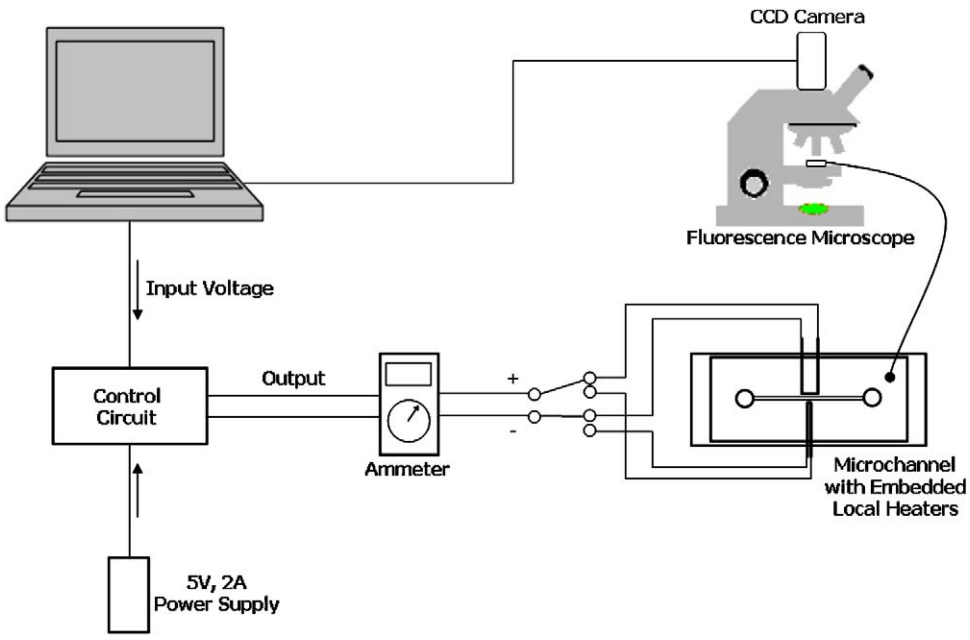

Fig. 1. Schematic of the experimental system.

heaters can be very costly and time consuming, and often these patterned microheater circuits cannot be used because they will block the observation of the channel under a microscope, and interfere with fluorescent-based optical measurements. Therefore, it is very important to find another method that costs less and can provide local heating on a chip, without blocking the observation of the microchannel.

Due to the size of microfluidic devices, aside from the fabrication, a major difficulty in evaluating microheaters is the determination of the resulting temperature field of the liquid in a microchannel. Some microreactors incorporate embedded thermocouples to measure temperature at predetermined locations [8]. The disadvantages of this method are that a thermocouple may affect the temperature field, and only temperatures at discrete locations are obtainable. Non-contact temperature measurement methods using fluorescent-labeled oligomers [22], temperature dependent fluorescent dyes [15,23,24], and reporter–quencher pairs [25] have been attempted, though they are not widely used and standardized.

Considering that poly(dimethylsiloxane) (PDMS) has been widely used in microfluidic systems, it is highly desirable to develop a low cost PDMS compatible microheater, so that it is possible to develop disposable biomedical chips with thermally controlled reactors.

In this work, we present a new microheater design by embedding resistance wires into a PDMS chip, and the results of a detailed experimental study of the heat transfer phenomena associated with this local heater in a microfluidic system. The thermal characteristics were measured by using the temperature-dependent fluorescent dye method. In the following sections, materials and experimental methods are described first. The capability of this kind of microheater is then demonstrated. Finally, the characteristics of the thermal response of the proposed heater are analyzed. Through a comparison with numerical analysis, the temperature response of the liquid sample controlled by the local heater is further elaborated.

2. Experimental section

A variety of experimental techniques have been developed to measure the liquid temperature inside microfluidic systems, such as backscatter interferometry [26], nuclear magnetic resonance (NMR) [27], Raman spectroscopy [28], and temperature sensitive probes (e.g., thermochromic liquid crystal [29], fluorescent dye [23,24], etc.). Temperature sensitive rhodamine B dye was used in our temperature measurements. In this microscale thermometry technique, rhodamine B's fluorescence intensity is measured and its relative variation is then converted into liquid temperature using the calibrated intensity versus temperature relationship [23,24]. In this work, an experimental system, as shown in Fig. 1, was developed to monitor the temperature by measuring the fluorescence intensity with a standard fluorescence microscope (TE2000, Nikon Inc.) and CCD camera (QImaging, Vancouver, BC, Canada). In the experiments, the microchannel was filled with an aqueous rhodamine B/buffer solution, and the intensity was monitored for various heater inputs. The images and local mean intensity values were stored for further processing.

2.1. Imaging and image processing

Imaging was performed using the fluorescence microscope and CCD camera referenced above. Excitation light of 480 nm was provided through a 1× microscope objective lens. The image capture time of the camera was once every 5 seconds for a constant applied heat flux, and once every second for thermal cycling. The individual exposure time was determined using the auto exposure function. The image resolution was

1392 × 1040 pixels, which captured a length of 9148 μm of the channel.

To correlate the fluorescence intensity to temperature, background and room temperature images of the channel were taken prior to each experiment. For each pixel, background substitution and normalization with room temperature yielded the normalized intensity, which was then converted to temperature using a previously determined calibration curve.

2.2. Microchannels and heater

The microchannels were fabricated in PDMS using the soft lithography technique. Briefly, masters containing the microchannel patterns were made by spin coating SU-8 photoresist on a clean glass slide. After a two-step soft bake (65 °C for 5 min and 95 °C for 15 min), the photoresist film was exposed to UV light for 7 s through a 3500 dpi transparent mask on which the desired channel structure had been printed. The transparency of the microchannel mask was generated by a high-resolution image-setter. Following another two step hard bake (65 °C for 1 min and 95 °C for 4 min), the slide was gently vibrated in the developer solution for 5 min to dissolve the unexposed photoresist, leaving a positive relief containing the microchannel pattern. A piece of resistance wire (0.25 mm diameter, Nickel–Chrome 60, Omega Engineering Inc.), bent into the appropriate heater shape (line or point), was then temporarily fixed to the master at a specified distance of 250 μm from the channel wall. Liquid poly(dimethylsiloxane) or PDMS was then poured over the master, degassed, and cured at 75 °C for approximately 3 hours. The negative PDMS cast of the microchannel pattern together with the resistor heater was then removed from the master, and two holes were punched to serve as reservoirs. Finally, the PDMS chip containing the microchannel and embedded resistance wires was permanently bonded to a glass slide by placing both sides to be bonded in a plasma cleaner (PDC-32G, Harrick Scientific, Ossiing, New York) and oxidizing them for 60 seconds. The assembly of the microheaters and microchannels was accomplished under a microscope for precise alignment of the microheater.

The final microchannel is shown schematically in Fig. 2(a) and (b) shows the area of the microchannel observed by the microscope. The microchannels were 50 μm deep, 550 μm wide, and 28 mm long. As shown in the figure, one heater was formed so that it had a short length parallel to the channel (approximately 2500 μm) and the other heater was formed so that it had a sharp angle pointing to the channel. For convenience, throughout the paper, the former is referred to as a line heater and the later as a point heater. The heaters constructed by this method can be very small and can heat the liquid sample from the side of the channel.

2.3. Chemicals

Rhodamine B (RhB) fluorescent dye was used due to its high temperature sensitivity (2–3%/K) [23]. Laser grade rhodamine B dye (Acros Organics, Pittsburgh, PA) was initially dissolved in pure water (Fisher Scientific Canada, Ottawa, ON) at a concentration of 1 mM and stored at −20 °C. Prior to the temperature measurements, the dye was further diluted to 50 μM in 25 mM sodium carbonate buffer solution at pH8.5. All solutions were filtered before use with 0.2 μm syringe filters (Whatman, Fisher Scientific Canada, Ottawa, ON).

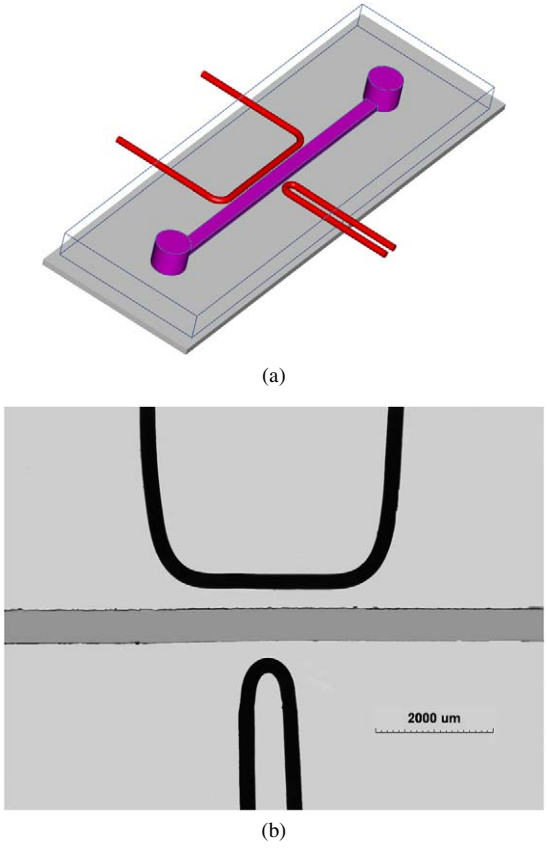

(a)

(b)

Fig. 2. (a) Schematic of microchannel with embedded resistance wire (b) Area of microchannel with embedded resistance wire observed by 1× objective.

2.4. Heater control

A circuit containing resistors, transistors, and a 5 V 2 A power supply controlled the current supplied to the resistance wire. The input voltage applied to the transistors was controlled by a data acquisition system (DAQPad-6020E, National Instrument Inc.) using LabVIEW software.

2.5. Temperature calibration

In order to determine the calibration curve to correlate normalized intensity with temperature, a thin film heater (Omega Engineering Inc.), metal substrate, and a thermocouple bound to the bottom of the substrate with conductive tape were used to provide a constant substrate temperature. A well containing a rhodamine B solution was clamped onto the substrate and the intensity of the well was monitored until it reached its steady state value, which corresponded to the measured substrate temperature.

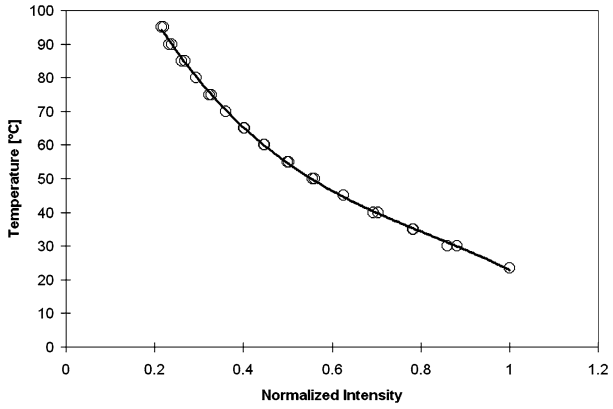

Fig. 3. Normalized intensity versus temperature calibration curve.

A calibration curve was produced, based on the method described above, and the resulting normalized intensity versus temperature is shown in Fig. 3. The average percent difference between measured normalized intensity data at a given temperature is 1.1%. A third order best fit polynomial is also shown, and has the equation

$$T = 149.15 - 317.84I + 323.41I^2 - 131.84I^3 \quad (2.1)$$

where T is the temperature and I is the intensity value subtract background and normalized by the intensity value at 23.5 °C. The calibration results were found to agree very well (within ±1 °C) with those presented by Ross et al. [23] for similar buffer concentration and pH.

3. Theoretical model and numerical simulation

Since the liquid sample heated in the microfluidic device has either very slow or no motion, it is reasonable to consider that the heat transfer is dominated by heat conduction. Therefore, in this paper, we neglected heat radiation and simply assumed that the heat transfer is heat conduction within the liquid sample, the solid channel wall, and the glass substrate. Here, we used a 3-D heat conduction model to describe the problem. The governing equation is,

$$\rho C_p \frac{\partial T}{\partial t} = \frac{\partial}{\partial x}\left(k\frac{\partial T}{\partial x}\right) + \frac{\partial}{\partial y}\left(k\frac{\partial T}{\partial y}\right) + \frac{\partial}{\partial z}\left(k\frac{\partial T}{\partial z}\right) + \dot{q} \quad (3.1)$$

where ρ is the density of the medium, C_p is the specific heat of the medium, k is the conductivity of the medium ($k_{\mathrm{PDMS}} = 0.15\ \mathrm{W\,m^{-1}\,K^{-1}}$, $k_{\mathrm{fluid}} = 0.60\ \mathrm{W\,m^{-1}\,k^{-1}}$, $k_{\mathrm{glass}} = 1.4\ \mathrm{W\,m^{-1}\,K^{-1}}$), T is the absolute temperature of the medium, and $\dot{q}$ is the heat source and only is non-zero at the region that represents the heating element, the electric resistance wire. A constant heat generation rate was applied at the location of the electric resistance wire.

To compare and verify the measured steady-state temperature profiles, a 3-D conduction simulation was completed using commercial Fluent CFD software. To reduce the computational load, a channel length of 10 mm was simulated. Free convection boundary conditions were imposed on the edges of the PDMS chip parallel to the channel and zero heat flux boundary conditions were imposed on the sides perpendicular to the channel.

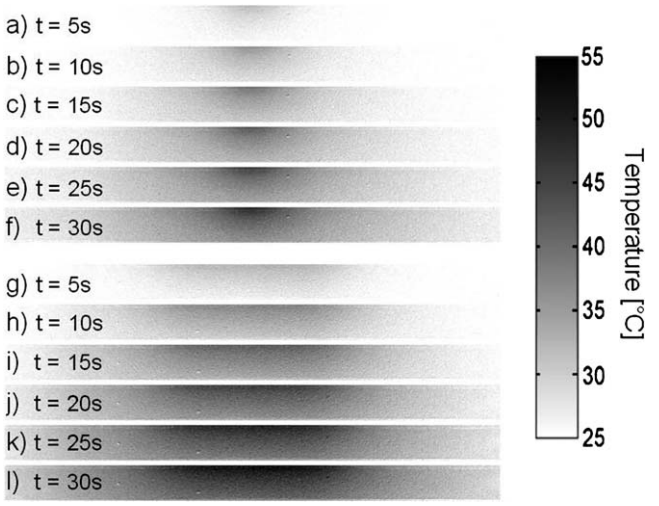

Fig. 4. Transient temperature contours of (a)–(f) point heater and (g)–(l) line heater under input power of 127 mW.

We also applied a free convection boundary condition on the top surface of the PDMS chip, and a constant temperature condition on the bottom of the base that the chip was sitting on during experiments.

4. Results and discussion

In order to assess the performance of the proposed local heaters in controlling the temperature of a liquid sample in the microfluidic system, the configuration shown in Fig. 2 was tested with a constant rate of the supplied heat and the thermal response of the fluid was monitored. Because the channel depth is much smaller than both the channel width and the microheater depth, the temperature difference in the depth direction is small and the monitored 2D fluorescence accurately represents the temperature field of the fluid within the microchannel.

Fig. 4 shows the transient thermal response of the two heaters embedded in the chip. In this figure, contour images (a)–(f) represent the transient temperature distribution in the liquid sample at different times, when a constant heat rate was applied using the point heater. Similarly, contour images (g)–(i) represent the transient temperature distribution resulting from the line heater. For each case, the time interval between adjacent images is 5 s. As shown in this figure, for both heaters, the temperature of the liquid near the heater region increased with time and was higher than that of the liquid away from the heater. This demonstrated that the resistance wire embedded in the PDMS chip can be used to locally control sample temperature, simply by optimizing the heater parameters. For the point heater, the liquid temperature started to increase at a point, and the heated liquid region spread out around the point heater in a semicircular shape. For the line heater, the liquid temperature started to increase at the wall of the microchannel, with a length equivalent to that of the line heater, and the heated liquid region spread out in an elongated elliptical shape. Therefore, the heater shape affects the directional heat generation rate and different shaped temperature distributions can be produced. This also indicates that the PDMS material enhances the local heat-

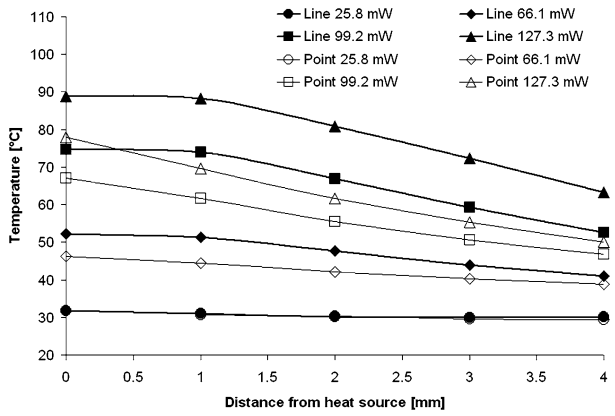

Fig. 5. Average steady-state temperature along the channel length versus distance from center of heater, for various input powers.

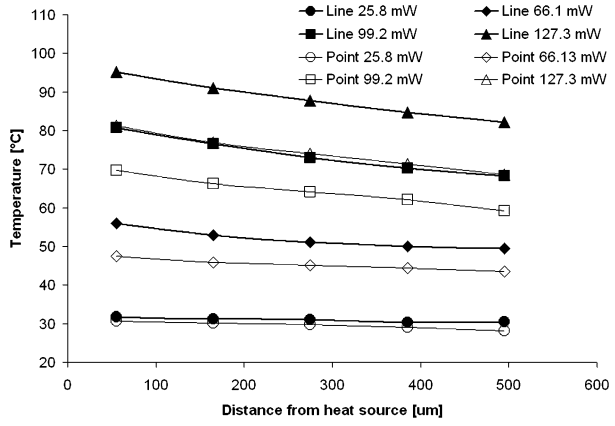

Fig. 6. Average steady-state temperature across the channel width versus distance from channel wall, for various input powers.

ing effect of the embedded heater, because the low conductivity of the PDMS hinders the heat dissipation from the fluid. This may be another advantage of using the PDMS embedded heater, since the thermal insulation in a microheater on a silicon wafer is not as effective as the PDMS. In chips tested in this study, the heater was located beside the channel at a distance of 250 μm. It is expected that the heating effect is stronger if the heater is placed closer to the channel of liquid.

To further analyze the performance of these two heaters, the steady-state temperature profiles resulting from each heater are depicted in Figs. 5 and 6.

Fig. 5 shows the average liquid temperature of a 450 μm by 450 μm area, versus distance from the center of the heater along the channel length. For both heaters, along the channel length the liquid temperature decreases with increasing distance from the heater. However, for the line heater, there is a uniform temperature region of a length similar to the heater length, followed by a nearly linear decrease in temperature. For the point heater, the temperature in the microchannel shows a linear decrease in temperature along the channel length. This quantifies the different steady-state temperature distributions that were achieved by using different heater configurations and shows the capabilities of each type of heater. For applications requiring a linear temperature gradient along the length of the channel, such as

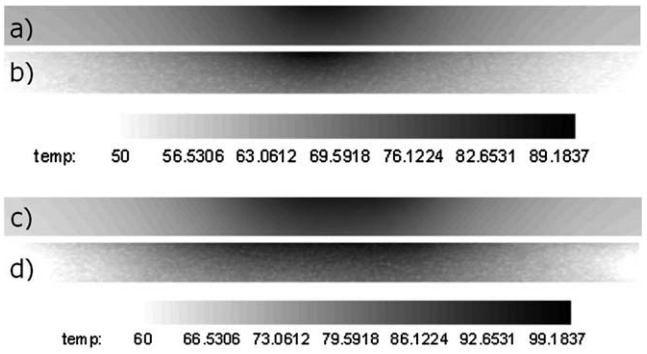

Fig. 7. Steady-state temperature contours for point heater (a) numerical (b) experimental and line heater (c) numerical (d) experimental.

microfluidic temperature gradient gel electrophoresis [30] and focusing [31,32], a point heater is suitable. A line heater is more appropriate for on-chip applications requiring a uniform steady state temperature field, such as chemical or protein synthesis, as it produces a region of constant temperature along the channel length. For both types of heater, a higher input power yields a larger temperature gradient across the liquid region. However, for the same power level, the line heater generates higher temperatures and larger temperature gradients. For the low power input case, the temperature difference in the liquid is very small when these two heaters are given the same input power.

Fig. 6 presents the average liquid temperature of a 2000 μm by 85 μm area, versus distance across the channel width, from the channel wall containing the embedded heater. Comparing Fig. 6 with Fig. 5, it is clearly shown that the thermal response of the liquid in the channel across the channel width is different from that along the channel length. For both kinds of heater, there is no uniform temperature region across the channel width and the liquid temperature decreases approximately linearly as the distance from the heater increases. The decreasing slope is larger when the input power to the heater is greater. The maximum temperature difference across the channel is about 10 °C and the corresponding temperature gradient is very high for a channel with a width of 550 μm. This implies that this new heater design can be used to provide the large temperature gradients required to study the response of proteins [33] or organisms [34] to a temperature field. On the other hand, for applications such as PCR requiring a more uniform temperature field, another heater can be added to the other side of channel to reduce the magnitude of the generated temperature gradient. For the same total input power rate, the line heater generated higher temperatures than the point heater, and this trend is similar to the temperature variations along the channel length. Higher temperature resulted from more heat transferring into the liquid, due to the larger heating area of the line heater.

Fig. 7 compares the experimentally and numerically determined steady-state temperature fields. It is shown that the experimental results generally agree well with the numerical simulation. The numerical simulation underestimated the heater effect slightly, but did generate the same shaped temperature profiles. The difference between the numerical and experimental results can be attributed to the different channel length used in the simulation and experiment, the approximation of the

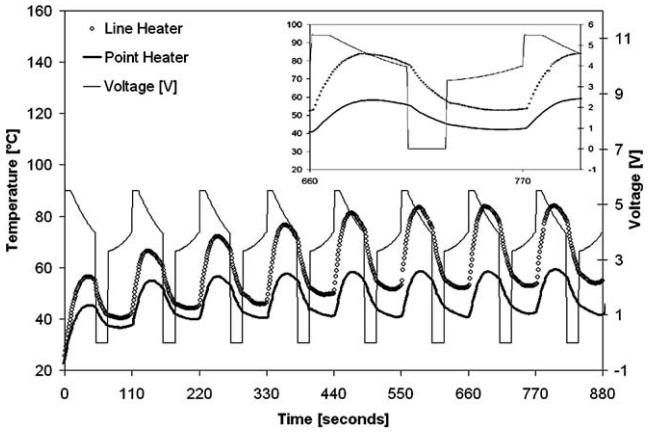

Fig. 8. Average thermal cycling temperatures achieved using the two heater configurations.

heater shape, and the choice of boundary conditions. These complexities emphasize the importance of developing an experimental method to evaluate the thermal field.

Fig. 8 shows the thermal cycling generated by controlling the heaters' power input. The voltage function driving the thermal cycling program is shown, and the temperature shown is the average liquid temperature of the 1400 μm by 500 μm area proximal to the heaters. This figure clearly indicates that steady-state thermal cycling was achieved after four cycles for both the pointer heater and line heater. Steady-state thermal cycling could also be achieved earlier, even by the first cycle, by using a hot start in which the high temperature level is maintained for a longer time to reduce the heat dissipation effects from the neighboring regions. One cycle consisted of 10 seconds of heating, 40 seconds of holding time at the higher temperature, 20 seconds of cooling (no heating power), and 40 seconds of holding time at the lower temperature. Holding temperatures were maintained for 30 seconds at $82 \pm 2\,^{\circ}\mathrm{C}$ and $54 \pm 1\,^{\circ}\mathrm{C}$ for the line heater and $57 \pm 1.5\,^{\circ}\mathrm{C}$ and $42.5 \pm 0.5\,^{\circ}\mathrm{C}$ for the point heater, by applying the same cubic voltage functions. The heating and cooling rates for the line heater are approximately double those of the point heater. This indicates that the microheaters and temperature monitoring method can also be applied to the development of the thermal cycling program required for PCR (polymerase chain reaction, a reaction for amplifying DNA) lab-on-chip applications. The thermal cycling profile generated by the designed heaters can be optimized to match the PCR requirements by tuning the temperature control as well as the heater configuration. Additionally, the uniformity of the temperature field required for PCR can be assessed using the temperature monitoring method outlined.

5. Conclusions

A new heater, constructed by a formed resistance wire embedded into a PDMS chip, is proven to be functional as a microheater for processes requiring incubation, temperature gradients, and thermal cycling. A point heater can provide localized thermal control and linear temperature gradients, while a line heater can provide a uniform temperature field over a greater channel length. Putting the heater at the side of the channel can generate a larger temperature gradient across the channel, without blocking the top or bottom view through the channel. This provides better conditions to monitor a bio-reaction/process under a microscope. The effectiveness of these on-chip microheaters was studied by using the temperature-dependent fluorescent dye method. The results proved that the fluorescent dye method is a good option for measuring the temperature field in microfluidic systems. The on-chip microheater formed by resistance wire embedded in a PDMS chip is effective, easy and inexpensive to fabricate, and has great potential for PDMS microfluidic systems.

Acknowledgement

Financial support from the National Sciences and Engineering Research Council (NSERC) of Canada, through a research grant to D. Li, is gratefully acknowledged.

References

[1] G.M. Whitesides, A.D. Stroock, Flexible methods for microfluidics, Phys. Today 54 (2001) 42–48.
[2] D.R. Reyes, D. Iossifidis, P. Aurous, A. Manz, Micro total analysis systems. 1. Introduction, theory, and technology, Anal. Chem. 74 (2002) 2623–2636.
[3] P. Aurous, D. Iossifidis, D.R. Reyes, A. Manz, Micro total analysis systems. 2. Analytical standard operations and applications, Anal. Chem. 74 (2002) 2637–2652.
[4] G.M. Whitesides, The 'right' size in nanobiotechnology, Nature Biotech. 21 (2003) 1161–1165.
[5] J.W. Hong, S.R. Quake, Integrated nanoliter systems, Nature Biotech. 21 (2003) 1179–1183.
[6] P. Watts, Chemical synthesis in micro reactors, Chemie Ingenieur Technik 76 (2004) 555–559.
[7] R.M. Tiggelaar, P.W.H. Loeters, P. van Male, R.E. Oosterbroek, J.G.E. Gardeniers, M.H.J.M. de Croon, J.C. Schouten, M.C. Elwenspoek, A. van den Berg, Thermal and mechanical analysis of a microreactor for high temperature catalytic gas phase reactions, Sensor Actuators A 112 (2004) 267–277.
[8] T. Yamamoto, T. Fujii, T. Nojima, A PDMS-glass hybrid microreactor array with embedded temperature control device. Application to cell-free protein synthesis, Lab Chip 2 (2002) 197–202.
[9] H. Nakamura, A. Tashiro, Y. Yamaguchi, M. Miyazaki, T. Watari, H. Shimizu, H. Maeda, Application of a microfluidic reaction system for CdSe nanocrystal preparation: their growth kinetics and photoluminescence analysis, Lab Chip 4 (2004) 237–240.
[10] J. West, B. Lillis, N. Cordero, E. Hurley, M.M. Sheehan, J.K. Collins, W. Lane, A. Mathewson, H. Berney, Electrolytic cell for access to genetic information, in: Proceedings of 2nd Annual Conference on Analytical Science, Ireland, 2002.
[11] I. Schneegab, R. Brautigam, J.M. Kohler, Miniaturized flow-through PCR with different template types in a silicon chip thermocycler, Lab Chip 1 (2001) 42–49.
[12] J. Yang, Y. Liu, C.B. Rauch, R.L. Stevens, R.H. Liu, R. Lenigk, P. Grodzinski, High sensitivity PCR assay in plastic micro reactors, Lab Chip 2 (2002) 179–187.
[13] P.G. Deng, Y.K. Lee, P. Cheng, The growth and collapse of a micro-bubble under pulse heating, Int. J. Heat Mass Transfer 46 (2003) 4041–4050.
[14] P.G. Deng, Y.K. Lee, P. Cheng, Micro bubble dynamics in DNA solutions, J. Micromech. Microeng. 14 (2004) 693–701.
[15] M. Gaitan, L.E. Locascio, Embedded microheating elements in polymeric micro channels for temperature control and fluid flow sensing, J. Res. Nat. Instit. Standards Technol. 109 (2004) 335–344.

[16] M. Baroncini, P. Placidi, G.C. Cardinali, A. Scorzoni, Thermal characterization of a microheater for micromachined gas sensors, Sensor Actuators A 115 (2004) 8–14.
[17] H. Yang, C.A. Choi, K.H. Chung, C.H. Jun, Y.T. Kim, An independent, temperature-controllable microelectrode array, Anal. Chem. 76 (2004) 1537–1543.
[18] N. Kitamura, Y. Hosoda, K. Ueno, S. Iwata, An application of plastic microchannel-microheater chips to a thermal synthetic reaction, Anal. Sci. 20 (2004) 783–786.
[19] C.W. Liu, C. Gau, B.T. Dai, Design and fabrication development of a micro flow heated channel with measurements of the inside micro-scale flow and heat transfer process, Biosensors and Bioelectronics 20 (2004) 91–101.
[20] N. Cordero, J. West, H. Berney, Thermal modelling of Ohmic heating microreactors, Microelectron. J. 34 (2003) 1137–1142.
[21] E. Garcia-Egiod, S.Y.F. Wong, B.H. Warrington, A Hantzsch synthesis of 2-aminothiazoles performed in a heated microreactor system, Lab Chip 2 (2002) 31–33.
[22] S. Jeon, J. Turner, S. Granick, Noncontact temperature measurement in microliter-sized volumes using fluorescent-labeled DNA oligomers, J. Amer. Chem. Soc. 125 (2003) 9908–9909.
[23] D. Ross, M. Gaitan, L.E. Locascio, Temperature measurement in microfluidic systems using a temperature-dependent fluorescent dye, Anal. Chem. 73 (2001) 4117–4123.
[24] D. Erickson, D. Sinton, D. Li, Joule heating and heat transfer in poly(dimethylsiloxane) microfluidic systems, Lab Chip 3 (2003) 141–149.
[25] R.E. Brewster, M.J. Kidd, M.D. Schuh, Optical thermometer based on the stability of a phosphorescent 6-bromo-2-naphthol/-cyclodextrin2 ternary complex, Chem. Commun. 12 (2001) 1134–1135.
[26] K. Swinney, D.J. Bornhop, Noninvasive picoliter volume thermometry based on backscatter interferometry, Electrophoresis 22 (2001) 2032–2036.
[27] M.E. Lacey, A.G. Webb, J.V. Sweedler, On-line temperature monitoring in a capillary electrochromatography frit using microcoil NMR, Anal. Chem. 74 (2002) 4583–4587.
[28] K.K. Liu, K.L. Davis, M.D. Morris, Raman spectroscopic measurement of spatial and temporal temperature gradients in operating electrophoresis capillaries, Anal. Chem. 66 (1994) 3744–3750.
[29] M. Chaudhari, T.M. Woudenberg, M. Albin, K.E. Goodson, Transient liquid crystal thermometry of microfabricated PCR vessel arrays, J. Microelectromech. Syst. 7 (1998) 345–355.
[30] J.S. Buch, C. Kimball, F. Rosenberger, W.E. Highsmith Jr, D.L. DeVoe, C.S. Lee, DNA mutation detection in a polymer microfluidic network using temperature gradient gel electrophoresis, Anal. Chem. 76 (2004) 874–881.
[31] D. Ross, L.E. Locascio, Microfluidic temperature gradient focusing, Anal. Chem. 74 (2002) 2556–2564.
[32] K.M. Balss, W.N. Vreeland, K.W. Phinney, D. Ross, Simultaneous concentration and separation of enantiomers with chiral temperature gradient focusing, Anal. Chem. 76 (2004) 7243–7249.
[33] M.A. Holden, P.S. Cremer, Microfluidic tools for studying the specific binding, adsorption, and displacement of proteins at interfaces, Annu. Rev. Phys. Chem. 56 (2005) 369–387.
[34] M.R. Clegg, S.C. Maberly, R.I. Jones, Behavioural responses of freshwater phytoplanktonic flagellates to a temperature gradient, European J. Phycol. 38 (2003) 195–203.